Oncogene (2014) **33,** 2577–2588

www.nature.com/onc

ORIGINAL ARTICLE

Repression of microRNA-768-3p by MEK/ERK signalling contributes to enhanced mRNA translation in human melanoma

CC Jiang[1,2], A Croft[1,3], H-Y Tseng[1,2], ST Guo[4], L Jin[5], P Hersey[5] and XD Zhang[1,2,4]

Increased global protein synthesis and selective translation of mRNAs encoding proteins contributing to malignancy is common in cancer cells. This is often associated with elevated expression of eukaryotic translation initiation factor 4 (eIF4E), the rate-limiting factor of cap-dependent translation initiation. We report here that in human melanoma downregulation of miR-768-3p as a result of activation of the mitogen-activated protein kinase kinase (MEK)/extracellular signal-regulated kinase (ERK) pathway has an important role in the upregulation of eIF4E and enhancement in protein synthesis. Melanoma cells displayed increased nascent protein production and elevated eIF4E expression, which was associated with the downregulation of miR-768-3p that was predicted to target the 3′-untranslated region of the eIF4E mRNA. Overexpression of miR-768-3p led to the downregulation of the endogenous eIF4E protein, reduction in nascent protein synthesis and inhibition of cell survival and proliferation. These effects were efficiently reversed when eIF4E was co-overexpressed in melanoma cells. On the other hand, introduction of anti-miR-768-3p into melanocytes upregulated endogenous eIF4E protein expression and increased global protein synthesis. Downregulation of miR-768-3p appeared to be mediated by activation of the MEK/ERK pathway, in that treatment of $BRAF^{V600E}$ melanoma cells with the mutant BRAF inhibitor PLX4720 or exposure of either $BRAF^{V600E}$ or wild-type BRAF melanoma cells to the MEK inhibitor U0126 resulted in the upregulation of miR-768-3p and inhibition of nascent protein synthesis. This inhibition was partially blocked in cells cointroduced with anti-miR-768-3p. Significantly, miR-768-3p was similarly downregulated, which was inversely associated with the expression levels of eIF4E in fresh melanoma isolates. Taken together, these results identify downregulation of miR-768-3p and subsequent upregulation of eIF4E as an important mechanism in addition to phosphorylation of eIF4E responsible for MEK/ERK-mediated enhancement of protein synthesis in melanoma.

Oncogene (2014) **33,** 2577–2588; doi:10.1038/onc.2013.237; published online 17 June 2013

Keywords: miR-768-3p; eIF4E; mRNA translation; melanoma; RAF/MEK/ERK

INTRODUCTION

Cancer cells require increased protein production to sustain their malignant characteristics such as enhanced survival and proliferation.[1–4] The rate of mRNA translation has an important role in regulating protein expression and is primarily controlled at the stage of translation initiation.[1–4] Initiation of translation of most mRNAs is mediated by the cap-dependent mechanism, whereas cap-independent initiation is involved in the translation of a subset of mRNAs, especially under cellular stress conditions.[1,3] Cap-dependent translation initiation is governed by the eukaryotic initiation factor (eIF) 4F (eIF4F) complex that consists of the cap-binding protein eIF4E, the RNA helicase eIF4A and the scaffolding protein eIF4G.[1–4] Among them, eIF4E is the rate-limiting factor that potentially influences the expression of almost every protein in cells.[1,5,6]

The activity of eIF4E is regulated by its availability that is controlled by the eIF4E inhibitory binding proteins (4E-BPs), in particular, 4E-BP1.[1,5,6] Hypophosphorylated 4E-BP1 shares the same binding motif with eIF4G and thus competes with eIF4G for binding to and sequestering eIF4E.[1,5,6] In addition, phosphorylation of eIF4E at serine 209 upon binding to eIF4G by mitogen-activated protein kinase signal-integrating kinase 1 (MNK1) and MNK2 enhances its activity.[5,7,8] Importantly, overexpression of eIF4E promotes cellular transformation and tumourigenesis.[9–11] This is associated with increased translation of various mRNAs encoding cancer-promoting proteins.[1,10–12] Indeed, eIF4E is expressed at increased levels in many types of cancers, such as those of the breast and colon,[13–15] which is often associated with disease progression and poor prognosis of patients.[1,13–15] However, the mechanism(s) responsible for the upregulation of eIF4E in cancer cells remains elusive.

MicroRNAs (miRs) regulate gene expression in a sequence-specific manner through binding to 3′-untranslated regions (UTRs) of target mRNAs, either targeting the transcripts for degradation or blocking their translation.[16,17] They can also inhibit translation by directly targeting the eIF4F complex.[18,19] The expression of miRs is frequently deregulated in cancer cells and many miRs are oncogenic or tumour suppressive.[17,20] In particular, a number of miRs such as miR-221/222 and miR-149* are known to regulate melanoma cell survival or proliferation.[21–25] Diverse mechanisms are involved in the regulation of miR expression in a tissue- and cell type-specific manner. These include genomic alterations, epigenetic changes and transcription factor-mediated transactivation or repression.[16,26,27]

A characteristic of human melanoma is oncogenic activation of the mitogen-activated protein kinase kinase (MEK)/extracellular

[1]Priority Research Centre for Cancer Research, University of Newcastle, Callaghan, NSW, Australia; [2]School of Medicine and Public Health, University of Newcastle, Callaghan, NSW, Australia; [3]Oncology and Immunology Unit, Calvary Mater Newcastle Hospital, Waratah, NSW, Australia; [4]Department of Molecular Biology, Shanxi Cancer Hospital and Institute, Taiyuan, Shanxi, People's Republic of China and [5]Kolling Institute for Medical Research, University of Sydney, St Leonards, NSW, Australia. Correspondence: Dr XD Zhang, School of Medicine and Public Health, Priority Research Center for Cancer Research; Cancer Research, LS3-49, Life Sciences Building, University of Newcastle, Callaghan, NSW 2308, Australia.
E-mail: Xu.Zhang@newcastle.edu.au
Received 1 November 2012; revised 8 April 2013; accepted 8 April 2013; published online 17 June 2013

signal-regulated kinase (ERK) pathway.[28,29] This stems primarily from activating mutations of BRAF, with the most common mutation being a glutamic acid for valine substitution at position 600 ($BRAF^{V600E}$).[28,29] Noticeably, a number of miRs such as miR-193a, miR-338 and miR-768-3p have been reported to be regulated by oncogenic activation of MEK/ERK signalling in melanoma.[30,31] Although activation of the MEK/ERK pathway is known to promote protein synthesis by phosphorylation of eIF4E through activation of MNK1 and MNK2,[1–4,7] we have found in this study that upregulation of the expression of eIF4E also has an important role in MEK/ERK-mediated enhancement of mRNA translation in melanoma. We demonstrate here that MEK/ERK-mediated upregulation of eIF4E is due to its inhibitory effect on the expression of miR-768-3p. The latter targets eIF4E and is commonly downregulated in melanoma cells.

RESULTS

eIF4E is upregulated in melanoma cells

Increased mRNA translation has an important role in the pathogenesis of cancer.[1–4] In line with this, the magnitude of nascent protein synthesis appeared significantly increased in cultured melanoma cells compared with melanocytes (Figures 1a and b). Similarly, the relative amount of polysome-associated mRNA in melanoma cells was also increased (Figure 1c). This was associated with increased expression and phosphorylation of the eIF4E protein (Figures 1d and e). The elevated levels of protein production and eIF4E expression and phosphorylation in melanoma cells compared with melanocytes was not due to the differences in culture conditions, in that Mel-RM and Mel-CV cells grown in melanocyte culture medium displayed even further increases, albeit moderately, in protein synthesis and eIF4E expression and phosphorylation. In contrast, when melanocytes were switched to melanoma cell culture medium, the levels of protein synthesis and eIF4E expression and phosphorylation were reduced (Supplementary Figure 1).

The role of eIF4E in increased protein synthesis in melanoma cells is confirmed by small RNA interference (siRNA) knockdown of eIF4E, which caused marked reduction in nascent protein synthesis in Mel-CV cells (Figures 1f and g). However, it displayed less pronounced effect in Mel-RM cells. This was conceivably due to the residual eIF4E protein that might remain adequate to drive mRNA translation as the endogenous eIF4E inhibitor 4E-BP1 was also downregulated when eIF4E was knocked down in the cells (Figure 1f).[32] Nonetheless, knockdown of eIF4E rendered Mel-RM cells more sensitive to 4EGI-1, a small molecule that inhibits the interaction between eIF4E and eIF4G (Figure 1h).[33] Collectively, these results indicate that mRNA translation is enhanced, which is at least, in part, due to the upregulation of eIF4E, in melanoma cells.

Contrary to its ~6-fold increases at the protein level (Figure 1e), the eIF4E transcript was elevated <2-folds and displayed comparable turnover rates in melanoma cells compared with melanocytes (Figures 2a and b). Moreover, the half-life time of the eIF4E protein did not appear to prolong in melanoma cells (Figures 2c and d). These data suggest that translational upregulation may have an important role in increased expression of eIF4E in melanoma cells.

MiR-768-3p is downregulated in melanoma cells

We sought to determine if miRNAs that commonly target transcripts to block their translation are involved in the regulation of eIF4E by comparing miRNA expression profiles between Mel-RM and Mel-CV melanoma cell lines and HEMn-MP and HEMn-DP melanocyte lines using TaqMan low-density array (Applied Biosystems, Mulgrave, VIC, Australia). Among miRNAs that were differentially expressed, a decrease in miR-768-3p, whose 'seed' region matched perfectly to a region (nucleotides 2645–2652) at the 3′-UTR of the eIF4E mRNA, in melanoma cells was one of the most pronounced (Genes-to-System Breast Cancer Database: http://www.itb.cnr.it/breastcancer//index.htm) (Figures 3a and b and Supplementary Table 1). This was subsequently confirmed in 10 melanoma cell lines (Figure 3c). In contrast, other miRNAs that are predicted to target eIF4E (MiRanda (http://www.microrna.org) and Target Scan (http://www.targetscan.org)) such as miR-150b and miR-382 did not significantly alter in expression in melanoma cells compared with melanocytes (Supplementary Table 1). Of importance, miR-768-3p was expressed at reduced levels in 48/50 of metastatic melanoma isolates relative to primary melanocytes (Figure 3d), suggesting that inhibition of miR-768-3p expression may have functional significance in melanoma biology *in vivo*.

Figure 1. Nascent protein synthesis is increased, and eIF4E is upregulated, in melanoma cells. (**a**) Representative flow cytometric histograms of quantitation of nascent protein synthesis using the Click-iT protein synthesis assay kit in HEMn-MP melanocytes and Mel-RM melanoma cells. Filled histograms: cells without labelling with metabolic labelling reagent; open histograms: cells were labelled with metabolic labelling reagent. MFI: mean fluorescence intensity. The data shown are representative of three individual experiments. (**b**) Quantitation of nascent protein synthesis in a panel of melanoma cell lines relative to the HEMn-MP and HEMn-DP melanocyte lines using the Click-iT protein synthesis assay kit as described in (**a**). The MFI of each sample was normalized against the corresponding sample without labelling with the metabolic labelling reagent. The relative magnitude of nascent protein synthesis of HEMn-MP was arbitrarily designated as 1. The data shown are the mean ± s.e. of three individual experiments. (**c**) Polysome fractions of HEMn-MP melanocytes and Mel-RM and Mel-CV melanoma cells were collected using sucrose-gradient centrifugation and were subjected to polysome profiling where the absorbance of each fraction was measured at 254 nm. The data shown are representative of three individual experiments. (**d**) Whole-cell lysates from melanocytes (HEMn-MP and HEMn-DP) and melanoma cells as indicated were subjected to western blot analysis of phosphorylated eIF4E, eIF4E and glyceraldehyde 3-phosphate dehydrogenase (GAPDH) (as a loading control). The data shown are representative of three individual experiments. (**e**) Comparison of eIF4E expression levels between melanocytes and melanoma cells as shown in (**d**). Levels of eIF4E were normalized to those of GAPDH. Quantitation of each band was determined using the NIH Image J software (NIMH, Bethesda, MD, USA). The mean eIF4E expression level of HEMn-MP and HEMn-DP melanocytes was arbitrarily designated as 1. The data shown are mean ± s.e. of three individual experiments. The average eIF4E expression levels in melanoma cells are ~6-fold higher than melanoctyes. (**f**) Mel-RM and Mel-CV cells were transfected with the control or eIF4E siRNA. After 24 h, whole-cell lysates were subjected to western blot analysis of eIF4E, 4E-BP1 and GAPDH (as a loading control). The data shown are representative of three individual experiments. (**g**) Mel-RM and Mel-CV cells were transfected with the control or eIF4E siRNA. After 24 h, cells were subjected to measurement of nascent protein synthesis using the Click-iT protein synthesis assay kit by flow cytometry. The MFI of each sample was normalized against the corresponding sample without labelling with the metabolic labelling reagent. The relative magnitude of nascent protein synthesis in cells from each line transfected with the control siRNA was arbitrarily designated as 1. The data shown are mean ± s.e. of three individual experiments. (**h**) Mel-RM cells were transfected with the control or eIF4E siRNA. After 24 h, cells were treated with 4EGI-1 (5 μM) for a further 24 h. Cells were then subjected to measurement of nascent protein synthesis using the Click-iT protein synthesis assay kit by flow cytometry. The MFI of each sample was normalized against the corresponding sample without labelling with the metabolic labelling reagent. The relative magnitude of nascent protein synthesis in cells transfected with the control siRNA without exposure to 4EGI-1 was arbitrarily designated as 1. The data shown are mean ± s.e. of three individual experiments.

MiR-768-3p downregulates eIF4E

As miR-768-3p overlaps with the small nucleolar RNA HBII-239,[34,35] we interrogated the potential interaction of this RNA with Argonaute (Ago) proteins, a core component of the RNA-induced silencing complex (RISC) by co-immunoprecipitation using an Ago (pan) antibody.[36] MiR-221 that is functionally verified in melanoma cells was included as a positive control,[21,23] and the small nuclear RNA U6, as a negative control.[37] Similar to miR-221, the majority of this RNA (more than 80% in comparison with the input in both Mel-RM and Mel-CV cells) was associated with Ago proteins, whereas, as expected, U6 was not enriched in the Ago precipitates (Figure 4a). These results indicate that this RNA is indeed processed into a mature miR (miR-768-3p) in melanoma cells.[36]

To verify that miR-768-3p targets eIF4E, we introduced luciferase reporter plasmids of the 3′-UTR of eIF4E into Mel-RM cells and HEMn-MP melanocytes (Figure 4b and Supplementary Figure 2). The reporter activity was markedly suppressed by the presence of the 3′-UTR of eIF4E in HEMn-MP, and to a lesser extent in Mel-RM cells, which was however reversed when the 3′-UTR was mutated (Figure 4b), suggesting that the 3′-UTR of eIF4E was inhibited by endogenous miR-768-3p. In support, cointroduction of anti-miR-768-3p into Mel-RM and HEMn-MP cells increased (Figure 4c), whereas the addition of miR-768-3p mimics further reduced the reporter activity (Figure 4d). Therefore, miR-768-3p targets the 3′-UTR of eIF4E in both melanoma cells and melanocytes. The fragment of DNA cloned into luciferase reporter plasmids was indeed present at the endogenous 3′-UTR of eIF4E in

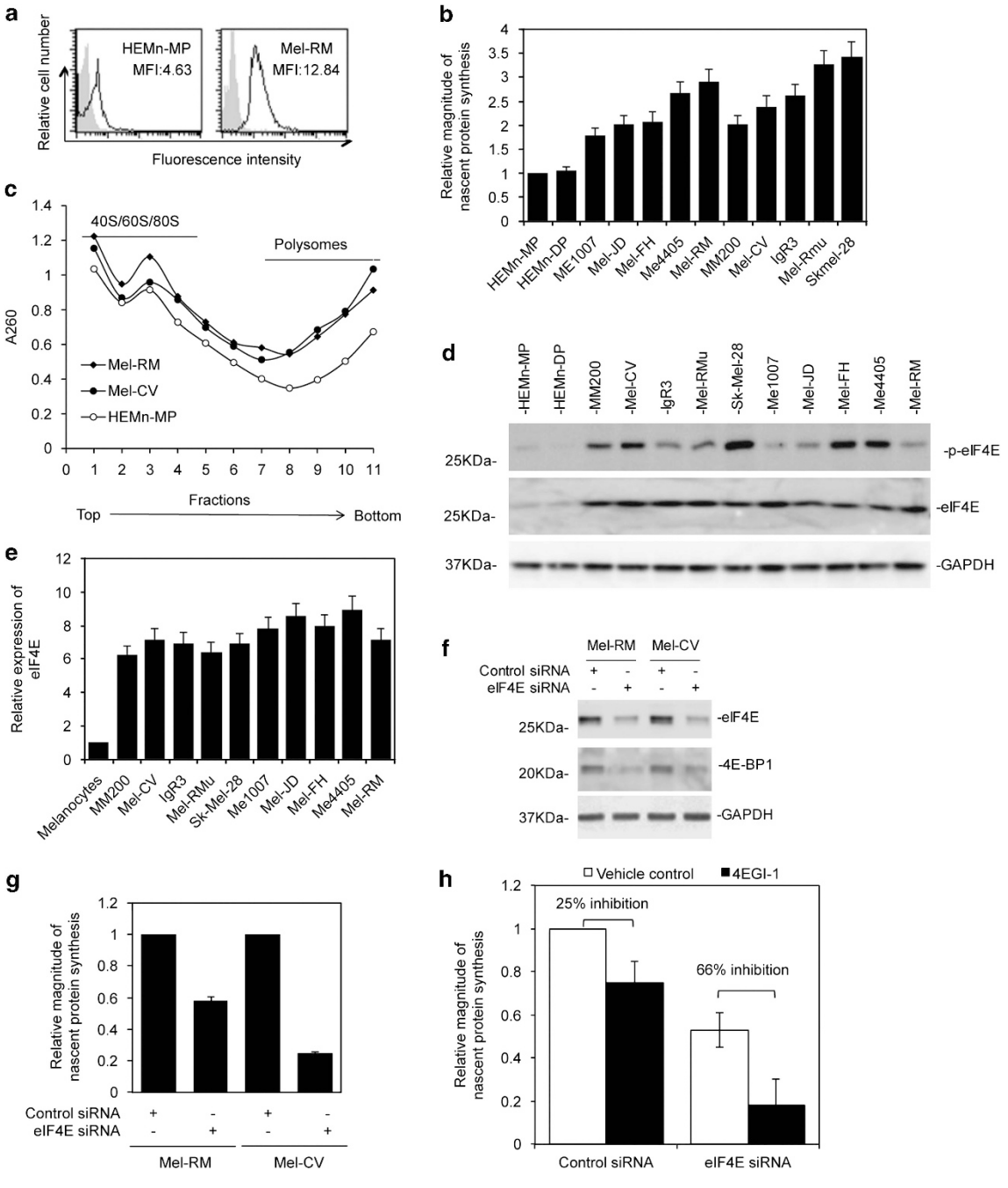

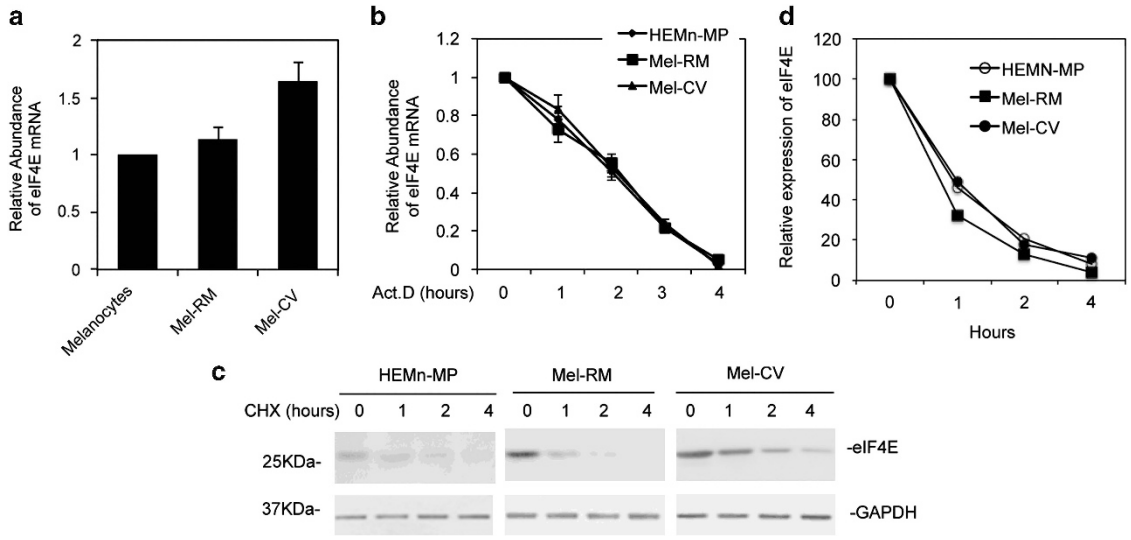

Figure 2. The increase in eIF4E expression in melanoma cells may be mediated by translational upregulation. (**a**) Total RNA from HEMn-MP melanocytes and Mel-RM and Mel-CV melanoma cells was subjected to qPCR analysis of eIF4E mRNA expression. The relative expression level of eIF4E mRNA in each sample was normalized against β-actin mRNA. The relative abundance of eIF4E mRNA in HEMn-MP melanocytes was arbitrarily designated as 1. The data shown are mean ± s.e. of three individual experiments. (**b**) HEMn-MP melanocytes and Mel-RM and Mel-CV melanoma cells were treated with actinomycin D (Act.D) (100 ng/ml) for indicated periods. Total RNA was subjected to qPCR analysis of eIF4E mRNA expression. The relative expression level of eIF4E mRNA in each sample was normalized against β-actin mRNA. The relative abundance of eIF4E mRNA in each cell line before treatment was arbitrarily designated as 1. The data shown are mean ± s.e. of three individual experiments. (**c**) Whole-cell lysates from HEMn-MP melanocytes, Mel-RM and Mel-CV melanoma cells with or without treatment with cycloheximide (CHX) (100 μg/ml) for indicated periods were subjected to western blot analysis of eIF4E and GPADH (as a loading control). The data shown are representative of three individual experiments. (**d**) Comparison of eIF4E expression levels in each cell line before and after treatment with cycloheximide as shown in (**c**). Levels of eIF4E were normalized to those of glyceraldehyde 3-phosphate dehydrogenase (GAPDH). Quantitation of each band was determined using the NIH Image J software. The eIF4E expression level of each cell line before treatment was arbitrarily designated as 100. The data shown are mean ± s.e. of three individual experiments.

Mel-RM and HEMn-MP cells as verified by polymerase chain reaction (PCR) analysis (Supplementary Figures 2 and 3).

Introduction of miR-768-3p mimics into Mel-RM cells downregulated the endogenous eIF4E protein levels, whereas introduction of anti-miR-768-3p into HEMn-MP resulted in an increase in the eIF4E protein expression (Figure 4e). These results substantiate that eIF4E is a *bona fide* target of miR-768-3p that is downregulated in melanoma cells. The endogenous levels of another two predicted miR-768-3p targets, Bcl-2 and ATF6, were not affected by the introduction of miR-768-3p mimics or anti-miR-768-3p (Supplementary Figure 4), suggesting that suppression of eIF4E by miR-768-3p is highly selective in melanoma cells.

We also examined representative fresh melanoma isolates sampled by relatively low ($n = 3$), intermediate ($n = 3$) and high ($n = 3$) levels of miR-768-3p for the expression of eIF4E. The results showed that melanomas with low miR-768-3p expression displayed relatively high levels of eIF4E, whereas intermediate and high miR-768-3p expression associated with progressively less eIF4E (Figure 4f). Therefore, the inhibitory effect of miR-768-3p on eIF4E *in vivo* is in accordance with the regulatory model identified *in vitro* (Figures 4c–f).

Downregulation of miR-768-3p contributes to increased nascent protein synthesis

Having established the role of miR-768-3p in the suppression of eIF4E, we examined whether it is involved in increased nascent protein synthesis in melanoma cells. Introduction of miR-768-3p into Mel-RM and Mel-CV cells led to decreased global protein production (Figure 5a), which recapitulated the effect of knockdown of eIF4E (Figure 1g). In contrast, introduction of anti-miR-768-3p into HEMn-MP melanocytes resulted in increased nascent protein synthesis, which could be abolished by the cointroduction of eIF4E siRNA (Figures 5b and c). These results indicate that downregulation of miR-768-3p has an important role in increased protein synthesis in melanoma cells through the upregulation of eIF4E.

MiR-768-3p is responsive to the MEK/ERK pathway

The MEK/ERK pathway that has an important role in the regulation of mRNA translation is constitutively activated in the majority of melanomas.[28,29] We therefore examined whether miR-768-3p is involved in MEK/ERK-mediated regulation of protein synthesis in melanoma cells. Comparison of miRNA expression profiles in Mel-CV ($BRAF^{V600E}$) cells before and after treatment with the mutant BRAF inhibitor PLX4720 showed that an increase in miR-768-3p (~8-fold) was among the most significant changes in miRNA expression (Figure 6a and Supplementary Table 2). This was confirmed in a panel of $BRAF^{V600E}$ melanoma cell lines (Figure 6b). Similarly, treatment with the MEK inhibitor U0126 caused increases in miR-768-3p in both $BRAF^{V600E}$ and wild-type BRAF melanoma cell lines (Figure 6c). These results suggest that the MEK/ERK pathway has an important role in the suppression of miR-768-3p in melanoma cells.

PLX4720 inhibited nascent protein production in $BRAF^{V600E}$ melanoma cells, whereas U0126 in both $BRAF^{V600E}$ and wild-type BRAF melanoma cells (Figure 6d). However, this inhibition was partially reversed in cells introduced with anti-miR-768-3p (Figure 6e), which in part recapitulated the inhibitory effect on protein synthesis afforded by knockdown of eIF4E (Figures 1g and 6f), indicating that suppression of miR-768-3p and subsequent upregulation of eIF4E is involved in enhancement of mRNA translation mediated by MEK/ERK. Taken together, results from the above studies identify a novel MEK/ERK-dependent, miR-768-3p-mediated signalling pathway that contributes to increased

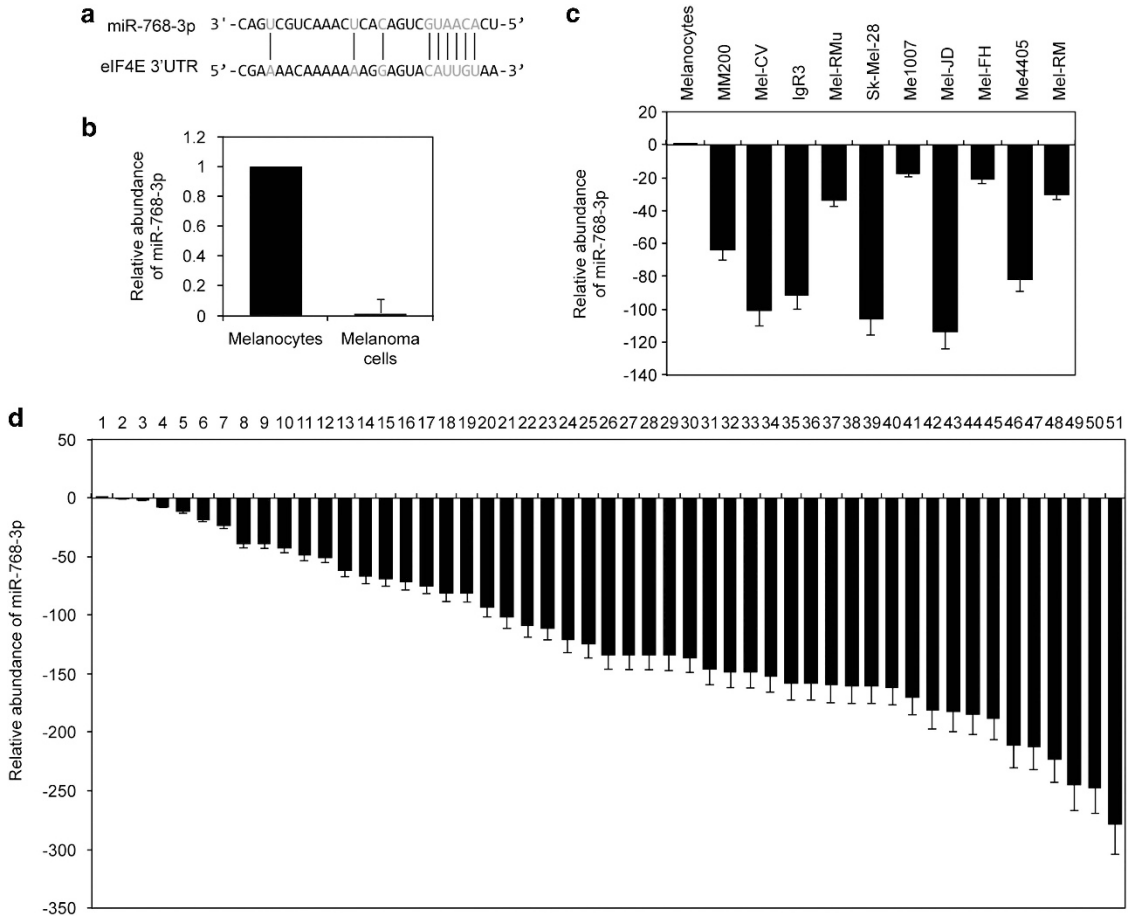

Figure 3. MiR-768-3p is downregulated in melanoma cells. (**a**) A schematic illustration of base-paring between miR-768-3p and the 3′-UTR of eIF4E mRNA. (**b**) Total miRNA from HEMn-MP and HEMn-DP melanocytes, Mel-RM and Mel-CV melanoma cells was subjected to miRNA expression profiling using TaqMan low-density array. The average abundance of miR-768-3p in HEMn-MP and HEMn-DP melanocytes was arbitrarily designated as 1. The relative abundance of miR-768-3p in melanoma cell lines was depicted. The data shown are mean ± s.e. of three individual experiments. (**c**) Total miRNA from HEMn-MP and HEMn-DP melanocytes and melanoma cells as indicated was subjected to qPCR analysis of miR-768-3p expression. The average level miR-768-3p in HEMn-MP and HEMn-DP melanocytes was arbitrarily designated as 1. The relative abundance of miR-768-3p in each melanoma cell line was depicted as folds of decreases (shown as negative values). The data shown are mean ± s.e. of three individual experiments. (**d**) Total miRNA from HEMn-MP and HEMn-DP melanocytes and 50 fresh melanoma isolates were subjected to qPCR analysis of miR-768-3p expression. The average level miR-768-3p in HEMn-MP and HEMn-DP melanocytes was arbitrarily designated as 1 (the first column: 1). The relative abundance of miR-768-3p in each isolate was depicted as folds of decreases (shown as negative values) (columns: 2–51). The data shown are mean ± s.e. of three individual experiments.

nascent protein synthesis in melanoma cells. As anticipated, PLX4720 downregulated the levels of phosphorylated eIF4E in Mel-CV ($BRAF^{V600E}$) cells, whereas U0126 in both Mel-CV and Mel-RM (wild-type BRAF) cells (Figure 6g). However, the kinetics of inhibition of eIF4E phosphorylation by PLX4720 and U0126 was more rapid than their inhibitory effects on the expression of eIF4E. Therefore, activation of MEK/ERK promotes mRNA translation by impinging on both eIF4E expression and its phosphorylation in a biphasic manner.

MiR-768-3p inhibits melanoma cell proliferation and survival

Although introduction of miR-768-3p mimics, alike knockdown of eIF4E, triggered apoptosis in a proportion of Mel-RM and Mel-CV cells (Figures 7a–c), inhibition of cell proliferation appeared to be the predominant consequence as shown in 5-bromo-2′-deoxyuridine (BrdU) incorporation and clonogenic assays (Figure 7d). In addition, cointroduction of miR-768-3p mimics and eIF4E siRNA further enhanced inhibition of cell survival and proliferation (Figure 7e). On the other hand, the inhibitory effect of miR-768-3p on cell proliferation was abolished in Mel-RM and Mel-CV cells overexpressing eIF4E (Figure 7f). Therefore, downregulation of miR-768-3p contributes to melanoma cell survival and proliferation by impinging on the expression of eIF4E.

To exclude possible off-target effects of the massive increase (a more than 15 000-fold increase in Mel-RM cells) in miR-768-3p expression, resulting from the introduction of miR-768-3p mimics, we introduced an miR-768-3p precursor-expressing construct into Mel-RM and Mel-CV cells. This led to a 24- and 34-fold increase in miR-768-3p in Mel-RM and Mel-CV cells, respectively (Supplementary Figure 5). Introduction of the construct caused apoptosis and inhibition of proliferation to a similar extent to that triggered by miR-768-3p mimics (Supplementary Figure 5), suggesting that the effect of miR-768-3p on melanoma cell survival and proliferation is specific.

To further validate the role of miR-768-3p in melanoma cell survival and proliferation, we introduced miR-768-3p mimics into two fresh metastatic melanoma isolates, Mel-JR and Mel-BE. As shown in Figure 7g, introduction of miR-768-3p mimics also resulted in reduced proliferation rates of these fresh melanoma isolates, which may reflect more closely melanoma cell responses to altered miR-768-3p expression *in vivo*.

DISCUSSION

In this report, we present evidence that miR-768-3p has an important role in inhibiting eIF4E expression and mRNA translation, and in regulating melanoma cell proliferation and survival. While its expression is commonly reduced in cultured melanoma cells and fresh melanoma isolates, introduction of exogenous miR-768-3p into melanoma cells resulted in the downregulation of eIF4E and reduction in nascent protein synthesis. This was associated with inhibition of cell proliferation and survival. Our results also reveal that downregulation of miR-768-3p in melanoma cells is mediated by activation of the MEK/ERK pathway.

Cancer cells require greater protein synthesis output to sustain their malignancy.[1–4] Consistent with this, we found that global mRNA translation and nascent protein production were increased in melanoma cells compared with melanocytes. Although we did not examine the translation rate of any particular mRNA, it is conceivable that translation of mRNAs encoding cancer-promoting proteins are accelerated in melanoma cells, as the increase in global protein synthesis is associated with an increase in the expression of eIF4E. While the latter is known to have the potential to mediate translation of almost every mRNA, its overexpression preferentially stimulates synthesis of a number of proteins that are associated with cancers such as c-MYC, cyclin-D1 and VEGF.[1,38–40] mRNAs encoding these proteins have highly structured 5′-UTRs, which result in their translation repression under normal conditions.[1,41] Nevertheless, these mRNAs respond more efficiently to elevated eIF4E.[1,38] Indeed, c-MYC, cyclin-D1 and

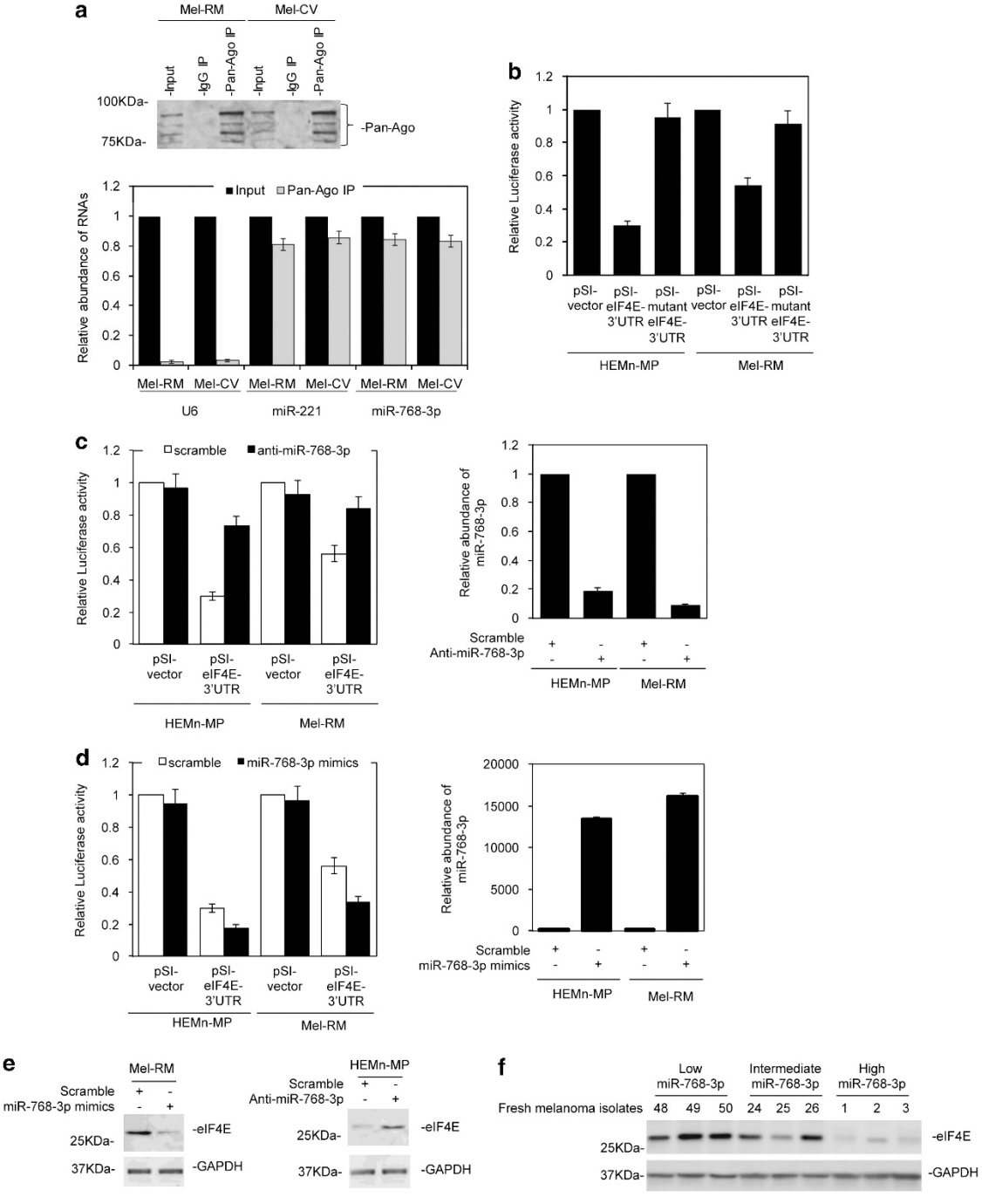

VEGF have all been reported to increase in expression in melanoma compared with nevus tissues.[38–40]

In experimental systems, overexpression of eIF4E promotes cancer development and progression, whereas inhibition of eIF4E suppresses malignancy.[42,43] Consistently, the expression of eIF4E is increased in many types of cancers including melanoma *in vivo*,[13–15,44] which is commonly correlated with disease progression and poor prognosis of patients, and is associated with resistance to therapeutic agents.[13–15,44] However, although it is well known that the eIF4E activity is regulated by its availability and phosphorylation, the mechanisms responsible for its upregulation remain less understood. We found in this study that the eIF4E protein was increased to a noticeably greater degree than its transcript in melanoma cells compared with melanocytes (~6 vs ~1.6 times), and that the stability of the protein and transcript remained similar between the two types of cells, suggesting that the increase in eIF4E is primarily mediated by translational regulation. We were thus promoted to explore the potential role of miRs in the regulation of eIF4E expression and identified downregulation of miR-768-3p as an important mechanism responsible for the upregulation of eIF4E in melanoma cells.

As miR-768-3p is located within the sequence of the small nucleolar RNA HBII-239,[34] its existence as an miR has been challenged and its entry has been removed from miRBASE. However, we found that miR-768-3p was associated with Ago proteins, a core component of the RNA-induced silencing complex, to the same extent as miR-221, a well-established miR that is increased in melanoma cells, indicating that miR-768-3p possesses the characteristics of a functional miR in melanoma cells.[36] In support, it has been recently reported that miRs could be generated by small nucleolar RNA.[35] It is conceivable that

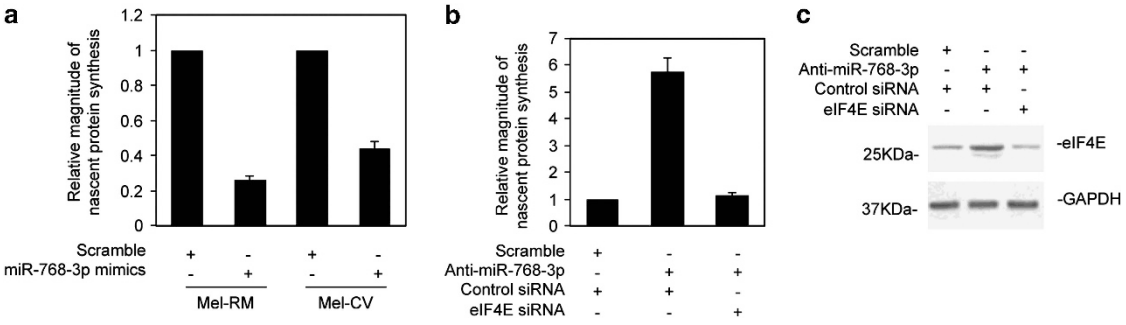

Figure 5. MiR-768-3p regulates nascent protein synthesis. (**a**) Mel-RM and Mel-CV cells were transfected with scrambled or miR-768-3p mimics. After 24 h, cells were subjected to measurement of nascent protein synthesis using the Click-iT protein synthesis assay kit by flow cytometry. The MFI of each sample was normalized against the corresponding sample without labelling with the metabolic labelling reagent. The relative magnitude of nascent protein synthesis in cells from each line transfected with the control scramble was arbitrarily designated as 1. The data shown are mean ± s.e. of three individual experiments. (**b**) HEMn-MP melanocytes were co-transfected with scrambled or anti-miR-768-3p oligonucleotides and the control or eIF4E siRNA. After 24 h, cells were subjected to measurement of nascent protein synthesis using the Click-iT protein synthesis assay kit by flow cytometry. The MFI of each sample was normalized against the corresponding sample without labelling with the metabolic labelling reagent. The relative magnitude of nascent protein synthesis in cells co-transfected with scrambled oligonucleotides and the control siRNA was arbitrarily designated as 1. The data shown are mean ± s.e. of three individual experiments. (**c**) HEMn-MP melanocytes were co-transfected with scrambled or anti-miR-768-3p oligonucleotides and the control or eIF4E siRNA. After 24 h, whole-cell lysates were subjected to western blot analysis of eIF4E and glyceraldehyde 3-phosphate dehydrogenase (GAPDH) (as a loading control). The data shown are representative of three individual western blot analyses.

Figure 4. MiR-768-3p targets eIF4E. (**a**) Upper panel: whole-cell lysates were subjected to immunoprecipitation with a mouse anti Ago (pan) antibody or purified mouse immunoglobulin G (IgG) (as a control). The resulting precipitates were subjected to western blot analysis of Ago proteins. Lower panel: Total miRNA isolated from the precipitates subjected to qPCR analysis of miR-768-3p, miR-221 (as a positive control) and U6 (as a negative control) expression. Total miRNA from each cell line was also analysed (input). The abundance of total miR-221, miR-768-3p and U6 in each cell line was arbitrarily designated as 1. The relative abundance of miR-221, miR-768-3p and U6 coprecipitated with Ago was depicted against 1. The data shown are mean ± s.e. of three individual experiments. The miRs were not detected in precipitates resulting from purified mouse IgG. (**b**) HEMn-MP melanocytes and Mel-RM melanoma cells were co-transfected with the indicated reporter constructs and luciferase plasmids. After 24 h, the reporter activity was measured using luciferase assays. Fold-activation values were measured relative to the levels of *Renilla* luciferase activity in cells transfected with vector alone (pSI-vector) and normalized by firefly luciferase activities. The data shown are the mean ± s.e. of three individual experiments. (**c**) Left panel: HEMn-MP melanocytes and Mel-RM melanoma cells were co-transfected with the indicated reporter constructs and *Renilla* luciferase plasmids. Scrambled or anti-miR-768-3p oligonucleotides were also co-transfected. After 24 h, the reporter activity was measured using luciferase assays. Fold-activation values were measured relative to the levels of *Renilla* luciferase activity in cells transfected with vector alone (pSI-vector) and scrambled oligonucleotides (scramble) and normalized by firefly luciferase activities. Right panel: qRT-PCR analysis of miR-768-3p in total miRNA from HEMn-MP and Mel-RM cells transfected with scrambled or anti-miR-768-3p oligonucleotides. The relative abundance of miR-768-3p in cells transfected with scrambled oligonucleotides (scramble) was arbitrarily designated as 1. The data shown are the mean ± s.e. of three individual experiments. (**d**) Left panel: HEMn-MP melanocytes and Mel-RM melanoma cells were co-transfected with the indicated reporter constructs and *Renilla* luciferase plasmids. Scrambled or miR-768-3p mimics were also co-transfected. After 24 h, the reporter activity was measured using luciferase assays. Right panel: qPCR analysis of miR-768-3p in total miRNA from HEMn-MP and Mel-RM cells transfected with scrambles or miR-768-3p mimics. The relative abundance of miR-768-3p in cells transfected with scrambled oligonucleotides (scramble) was arbitrarily designated as 1. The data shown are the mean ± s.e. of three individual experiments. (**e**) Left panel: Mel-RM melanoma cells were transfected with scrambled or miR-768-3p mimics oligonucleotides. After 24 h, whole-cell lysates were subjected to western blot analysis of eIF4E and glyceraldehyde 3-phosphate dehydrogenase (GAPDH) (as a loading control). Right panel: HEMn-MP melanocytes were transfected with scrambled or anti-miR-768-3p. After 24 h, whole-cell lysates were subjected to western blot analysis of eIF4E and GAPDH (as a loading control). The data shown are representative of three individual western blot analyses. (**f**) Whole-cell lysates from fresh melanoma isolates sampled by expression of relatively high, intermediate and low levels of miR-768-3p as shown in Figure 3d were subjected to western blot analysis of eIF4E and GAPDH (as a loading control). The data shown are representative of three individual western blot analyses.

miR-768-3p is processed into a mature miR through a non-canonical miR biogenesis pathway as proposed by others.[35]

The expression and functional importance of miRs in melanoma have been studied extensively in recent years.[21–25] Not only a number of miRs such as miR-211 have been found to be differentially expressed between melanocytes and melanoma cells[23,25] but also changes in the expression of a number of miRs have been demonstrated to be associated with melanoma progression and invasion.[23–25] We have also previously shown that miR-149* protects against apoptosis by stabilizing Mcl-1 via targeting glycogen synthase kinase 3α (GSK3α) in melanoma cells under endoplasmic reticulum stress.[22] Although inhibition of mRNA translation is a common mechanism by which an miR regulates its target gene expression,[16–18] our results reveal that miR-768-3p

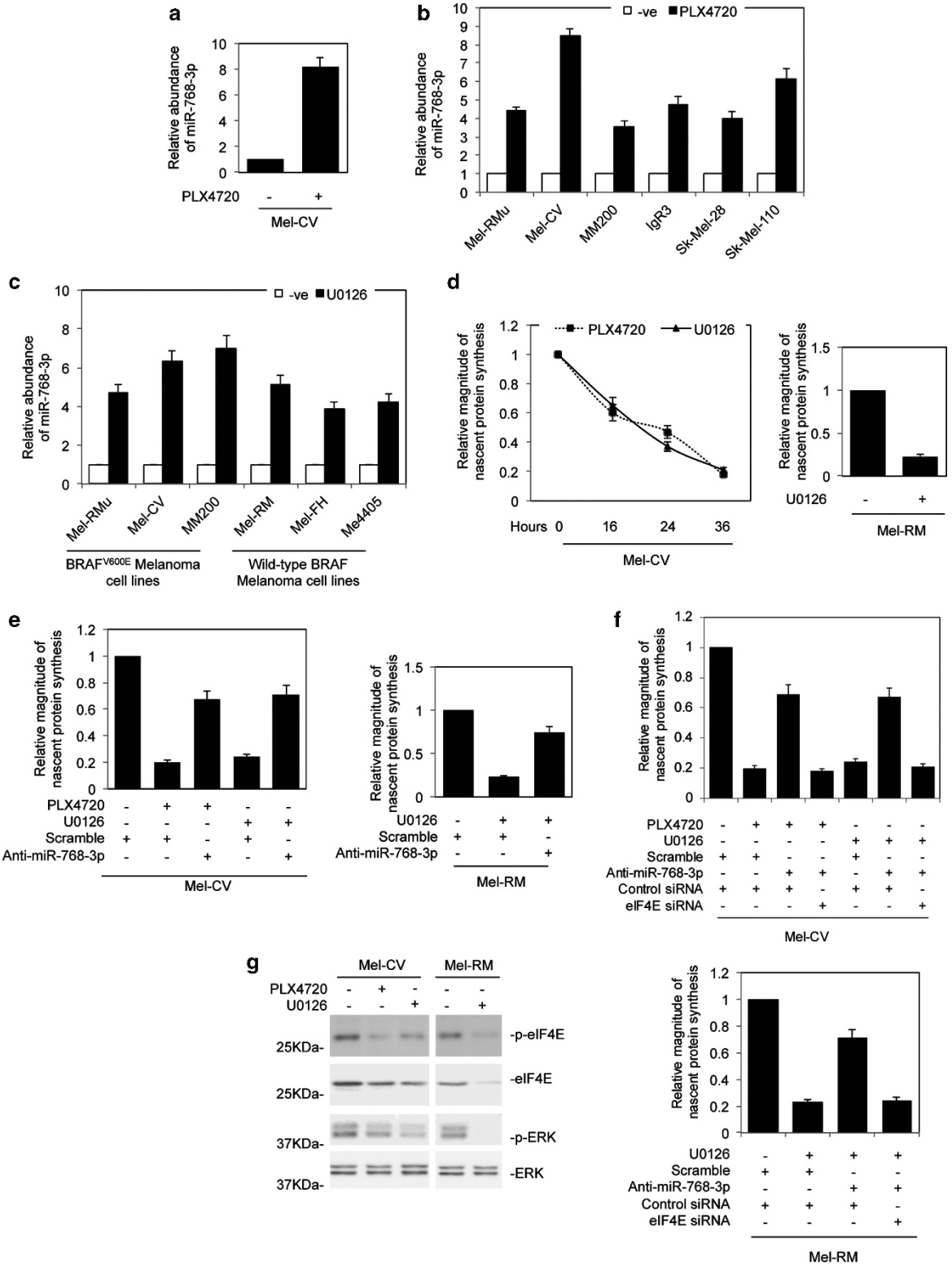

inhibits global protein synthesis by targeting eIF4E in melanoma cells. Targeting eIF4E by miR-768-3p appeared to be highly selective, in that the expression of Bcl-2 and ATF6, both of which are predicted targets of miR-768-3p, did not respond to overexpression or inhibition of miR-768-3p. Regulation of target expression by miRs is known to be tissue- and cell type-specific.[17]

The expression of miRs can be regulated by diverse mechanisms. These include genetic alterations, epigenetic changes and transcription factor-mediated transactivation or repression.[17,20] Of interest, many miRs are associated with signalling pathways important for the pathogenesis of melanoma. For example, miR-221/222 has been identified as regulators of c-KIT, whereas miR-137 and miR-148 as regulators of microphthalmia-associated transcription factor.[21,45,46] In particular, it has been recently reported that a number of miRs such as miR-193a, miR-338 and miR-768-3p are subjected to regulation by oncogenic activation of MEK/ERK signalling in melanoma.[30,31] Our finding that suppression of miR-768-3p by MEK/ERK contributes to enhanced mRNA translation through the upregulation of eIF4E indicates that miR-768-3p is a build-in component of the MEK/ERK pathway in melanoma cells. Therefore, activation of MEK/ERK signalling enhances protein synthesis not only by phosphorylating eIF4E vial activation of MNK1 and MNK2[1–4,7] but also through the upregulation of eIF4E expression.

Of note, miR-768-3p is embedded within intron 12 of the human gene encoding adaptor-related protein complex 1, gamma 1 subunit (AP1G1),[47] which was also increased by inhibition of MEK (Supplementary Figure 6), suggesting that miR-768-3p may be regulated along with the *AP1G1* gene in response to MEK/ERK signalling. However, the exact mechanism involved and the functional significance of the regulation of APIG1 by MEK/ERK remains to be investigated. APIG1 is known to have an important role in protein transportation mediated by clathrin-coated vesicles.[48]

The functional significance of miR-768-3p in melanoma was demonstrated by inhibition of cell survival and proliferation with its overexpression, which was also echoed by its downregulation in fresh melanoma isolates and the negative association between its expression levels and the levels of eIF4E. Multiple molecules conceivably contribute to the regulation of melanoma cell survival and proliferation by miR-768-3p, such as c-MYC and cyclin D1, which are sensitive to changes in the expression levels of eIF4E.[33,38–41] Targeting eIF4E is in development for clinical use in the treatment of cancer.[3,49] Our results suggest that restoration of the expression of miR-768-3p may be a useful alternative strategy for inhibition of eIF4E in melanoma. As a precedent, replacement therapy has been shown to be efficacious in a mouse model of colon cancer for miR-145 and miR-33a.[50] With continuing investigations into *in vivo* delivery systems for miRs, this approach is likely to be achievable.

MATERIALS AND METHODS

Cell culture and reagents

The human melanoma cell lines used have been described previously and are summarized in Supplementary Table 3.[51] They were cultured in Dulbecco's modified Eagle's medium containing 5% foetal calf serum (Commonwealth Serum Laboratories, Melbourne, VIC, Australia). The melanocyte lines HEMn-MP and HEMn-DP and melanocyte culture medium (M-254) were purchased from Banksia Scientific (Bulimba, QLD, Australia). Antibodies against p-eIF4E, eIF4E, p-ERK and the eIF4E inhibitor 4EGI-1 were purchased from Santa Cruz Biotechnology (Santa Cruz, CA, USA). Antibodies against 4E-BP1 and ERK were purchased from Cell Signalling Technology (Beverly, MA, USA). PLX4720 was provided by Plexxikon Inc. (Berkeley, CA, USA), which was dissolved in dimethylsulphoxide and made up in stock solutions of 4 mM. The MEK inhibitor U0126 was purchased from Promega (Madison, WI, USA). Mature hsa-miR-768-3p mimics and anti-miR-768-3p were purchased from Applied Biosystems (Mulgrave, VIC, Australia). Human fresh melanoma isolates were prepared according to a published method.[52] Studies using human tissues

Figure 6. MiR-768-3p is responsive to the MEK/ERK pathway. (**a**) Total miRNA from Mel-CV cells ($BRAF^{V600E}$) with or without treatment with PLX4720 (5 μm) for 24 h was subjected to miRNA expression profiling using TaqMan low-density array. The average abundance of miR-768-3p in cells without treatment was arbitrarily designated as 1. The data shown are mean ± s.e. of three individual experiments. (**b**) Total miRNA from cells of a panel of $BRAF^{V600E}$ melanoma cell lines with or without treatment with PLX4720 (5 μm) as indicated was subjected to qPCR analysis of miR-768-3p expression. The average abundance of miR-768-3p in cells of each line without treatment was arbitrarily designated as 1. The data shown are mean ± s.e. of three individual experiments. (**c**) Total miRNA from cells of a panel of melanoma cell lines with different BRAF mutational status as indicated with or without treatment with U0126 (20 μm) was subjected to qPCR analysis of miR-768-3p expression. The average abundance of miR-768-3p in cells of each line without treatment was arbitrarily designated as 1. The data shown are mean ± s.e. of three individual experiments. (**d**) Left panel: Mel-CV cells with or without treatment with PLX4720 (5 μm) or U0126 (20 μm) for indicated periods were subjected to measurement of nascent protein synthesis using the Click-iT protein synthesis assay kit by flow cytometry. The MFI of each sample was normalized against the corresponding sample without labelling with the metabolic labelling reagent. The relative magnitude of nascent protein synthesis in cells without treatment was arbitrarily designated as 1. Right panel: Mel-RM cells with or without treatment with U0126 (20 μm) for 24 h were subjected to measurement of nascent protein synthesis using the Click-iT protein synthesis assay kit by flow cytometry. The relative magnitude of nascent protein synthesis in cells without treatment was arbitrarily designated as 1. The data shown are mean ± s.e. of three individual experiments. (**e**) Left panel: Mel-CV cells were transfected with scrambled or anti-miR-768-3p oligonucleotides. After 24 h, cells were treated with PLX4720 (5 μm) or U0126 (20 μm) for a further 24 h. Cells were then subjected to measurement of nascent protein synthesis using the Click-iT protein synthesis assay kit by flow cytometry. The MFI of each sample was normalized against the corresponding sample without labelling with the metabolic labelling reagent. The relative magnitude of nascent protein synthesis in Mel-CV cells transfected with scrambles without treatment was arbitrarily designated as 1. Right panel: Mel-RM cells were transfected with scrambled or anti-miR-768-3p oligonucleotides. After 24 h, cells were treated with U0126 (20 μm) for a further 24 h. Cells were then subjected to measurement of nascent protein synthesis using the Click-iT protein synthesis assay kit by flow cytometry. The MFI of each sample was normalized against the corresponding sample without labelling with the metabolic labelling reagent. The relative magnitude of nascent protein synthesis in Mel-RM cells transfected with scramble without treatment was arbitrarily designated as 1. The data shown are mean ± s.e. of three individual experiments. (**f**) Upper panel: Mel-CV cells were co-transfected with scrambled or anti-miR-768-3p oligonucleotides and the control or eIF4E siRNA. After 24 h, cells were treated with PLX4720 (5 μm) or U0126 (20 μm) for a further 24 h. Cells were then subjected to measurement of nascent protein synthesis using the Click-iT protein synthesis assay kit by flow cytometry. The MFI of each sample was normalized against the corresponding sample without labelling with the metabolic labelling reagent. The relative magnitude of nascent protein synthesis in Mel-CV cells transfected with scramble and the control siRNA without treatment was arbitrarily designated as 1. Lower panel: Mel-RM cells were co-transfected with scrambled or anti-miR-768-3p oligonucleotides and the control or eIF4E siRNA. After 24 h, cells were treated with U0126 (20 μm) for a further 24 h. Cells were then subjected to measurement of nascent protein synthesis using the Click-iT protein synthesis assay kit by flow cytometry. The MFI of each sample was normalized against the corresponding sample without labelling with the metabolic labelling reagent. The relative magnitude of nascent protein synthesis in Mel-RM cells transfected with scramble and the control siRNA without treatment was arbitrarily designated as 1. The data shown are mean ± s.e. of three individual experiments. (**g**) Whole-cell lysates from Mel-CV cells with or without treatment with PLX4720 (5 μm) or U0126 (20 μm) for 24 h and Mel-RM cells with or without treatment with U0126 (20 μm) for 24 h were subjected to western blot analysis of phosphorylated eIF4E (p-eIF4E), eIF4E, phosphorylated ERK (p-ERK) and ERK. The data shown are representative of three individual experiments.

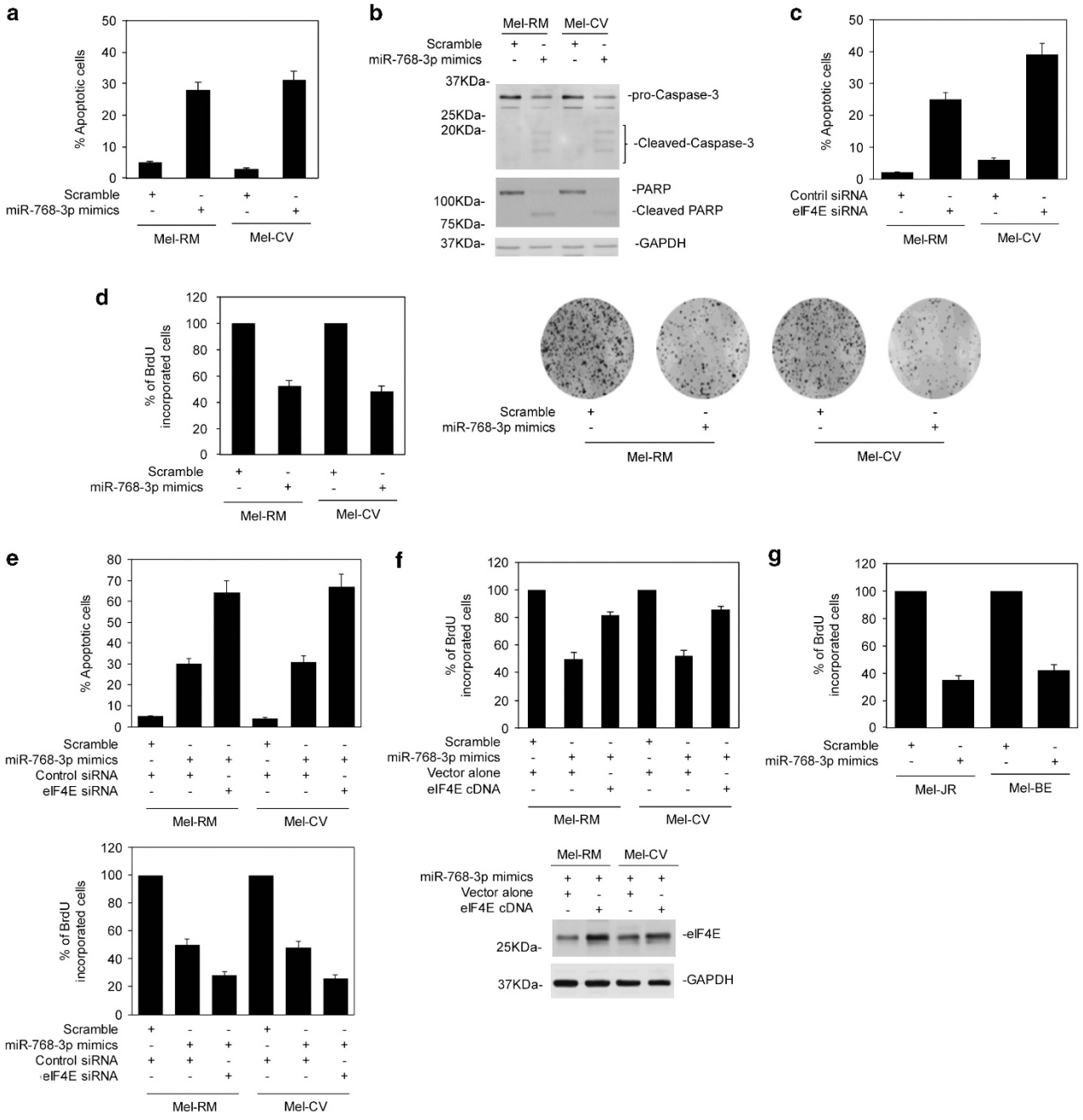

Figure 7. MiR-768-3p inhibits melanoma cell proliferation and survival. (**a**) Mel-RM and Mel-CV cells were transfected with scrambled or miR-768-3p mimics. After 48 h, cells were subjected to quantitation of apoptosis by measurement of sub-G1 DNA content. The data shown are mean ± s.e. of three individual experiments. (**b**) Mel-RM and Mel-CV cells were transfected with scrambled or miR-768-3p mimics. After 48 h, whole-cell lysates were subjected to western blot analysis of caspase-3, poly (ADP-ribose) polymerase (PARP) and glyceraldehyde 3-phosphate dehydrogenase (GAPDH) (as a loading control). The data shown are representative of three individual experiments. (**c**) Mel-RM and Mel-CV cells were transfected with the control or eIF4E siRNA. After 48 h, cells were subjected to quantitation of apoptosis by measurement of sub-G1 DNA content. The data shown are mean ± s.e. of three individual experiments. (**d**) Left panel: Mel-RM and Mel-CV cells were transfected with scrambled or miR-768-3p mimics. After 48 h, cells were subjected to proliferation assays using the BrdU incorporation method. The data shown are mean ± s.e. of three individual experiments. Right panel: Mel-RM and Mel-CV cells were transfected with scrambled or miR-768-3p mimics. After 24 h, viable cells (2000 cells per well in 6-well plates) were allowed to grow for 12 days before being fixed with methanol and stained with crystal violet. The data shown are representative of three individual experiments. (**e**) Upper panel: Mel-RM and Mel-CV cells were co-transfected with scrambled or miR-768-3p mimics and the control or eIF4E siRNA. After 48 h, cells were subjected to quantitation of apoptosis by measurement of sub-G1 DNA content. Lower panel: Mel-RM and Mel-CV cells were co-transfected with scrambled or miR-768-3p mimics and the control or eIF4E siRNA. After 48 h later, cells were subjected to proliferation assays using the BrdU incorporation method. The data shown are mean ± s.e. of three individual experiments. (**f**) Upper panel: Mel-RM and Mel-CV cells were co-transfected with scrambled or miR-768-3p mimics and vector alone or eIF4E cDNA. After 48 h, cells were subjected to proliferation assays using the BrdU incorporation method. The data shown are mean ± s.e. of three individual experiments. Lower panel: Mel-RM and Mel-CV cells were co-transfected with miR-768-3p mimics and vector alone or eIF4E cDNA. After 48 h, whole-cell lysates were subjected to western blot analysis of eIF4E and GAPDH (as a loading control). The data shown are representative of three individual experiments. Mel-JR and Mel-BE fresh melanoma isolates were transfected with scrambles or miR-768-3p mimics. After 48 h, cells were subjected to proliferation assays using the BrdU incorporation method. The data shown are mean ± s.e. of three individual experiments.

were approved by the Human Research Ethics Committee of University of Newcastle.

Nascent protein synthesis

Nascent protein synthesis was detected by the Click-iT protein synthesis assay kit according to the manufacturer's instruction (Life Technologies, Mulgrave, VIC, Australia). Briefly, cells were seeded at a density of 6×10^5 per well in a 6-well plate. After 24 h, cells were washed with warm phosphate-buffered saline (PBS) and incubated with methionine-free medium for 1 h at 37 °C. Fifty micromolar metabolic labelling reagent was then added, followed by incubating at 37 °C for 3 h. Cells were then scraped off into fluorescence-activated cell sorter tubes and washed with PBS and fixed with 4% paraformaldehyde, followed by permeabilization in PBS with supplemented with 0.1% saponin and 1% bovine serum albumin for 15 min. Permeabilized cells were then incubated with Click-iT reaction cocktail (Life Technologies) for 30 min at room temperature in dark. Cells were finally stained with Alexa Fluor 488 azide, followed by flow cytometry analysis. The mean fluorescence intensity (MFI) of each sample was corrected by extracting the background MFI detected in the corresponding sample without labelling with the metabolic labelling reagent. The relative magnitude of nascent protein synthesis in each sample represented by its MFI was then normalized against the MFI of the control sample in each experiment.

Polysome profiling

Polysome profiling was performed as reported previously.[53] Briefly, cells were seeded at a density of 7.5×10^6 cells in a T150 flask. After 24 h, cells were washed with PBS and incubated in 0.1 mg/ml cycloheximide (Sigma-Aldrich, Castle Hill, NSW, Australia) in PBS for 3 min at 37 °C. Cells were washed two times with PBS containing CHX (0.1 mg/ml) and lysed in RNA lysis buffer. Nuclei were subsequently removed by centrifugation, and cell debris was further removed from the supernatant. The lysate was layered onto 10-ml continuous sucrose gradients. After 90 min of centrifugation at 39 000 r.p.m. in an SW41-Ti rotor at 4 °C, the absorbance at 254 nm was measured continuously as a function of gradient depth.

BrdU incorporation

BrdU incorporation assays were performed by using FITC BrdU Flow Kit (BD Biosciences, North Ryde, NSW, Australia). Briefly, 10 μl BrdU solution was added into the tissue culture medium followed with desired treatment. Cells were then harvested and analysed using a flow cytometer.

Apoptosis

Quantitation of apoptotic cells was carried out by measurement of sub-G1 DNA content using propidium iodide on a flow cytometer as described elsewhere.[51,52]

Western blot analysis

Western blot analysis and quantitation of protein bands were carried out as described previously.[46,48]

Co-immunoprecipitation of Ago and miRs

Co-immunoprecipitation of Ago and miRs was carried out as described by others.[36] Briefly, 200 μl of MagnaBind goat anti-mouse immunoglobulin G Magnetic Beads (Thermo Fisher Scientific, Scoresby, VIC, Australia) was washed with PBS and incubated with 10 μg of a mouse anti-pan-Ago antibody (MABE56; Millipore, Kilsyth, VIC, Australia) or purified mouse normal immunoglobulin G (Santa Cruz Biotechnology) for 2 h at 4 °C. The beads were then added into the 400 μl of whole-cell lysates and incubated overnight at 4 °C, followed by washing three times with 1% Nonidet P-40 buffer. The beads were then divided equally into two parts. Proteins from half of the beads were eluted in 2 × sodium dodecyl sulphate sample buffer, followed by sodium dodecyl sulphate–polyacrylamide gel electrophoresis and western blot analysis of Ago. The other half of the beads was processed for RNA isolation using QIAzol, followed by quantitative reverse transcription and real-time PCR (qPCR) analysis of miRs.

TaqMan low-density array miR array

miRNA array was performed using TaqMan TaqMan low-density array card (Applied Biosystems). Briefly, miRNA was purified by using miRNeasy Mini Kit (Qiagen, Chadstone Centre, VIC, Australia). Purified miRNA was reversed transcribed using the Megaplex Reverse transcription primer pool (Applied Biosystems). Hundred nanogram cDNA was mixed with TaqMan Universal PCR Master Mix and then loaded onto the TaqMan low-density array card followed with qPCR analysis using an ABI Fast 7900HT sequence detection system (Applied Biosystems). Analysis of TaqMan low-density array data (Applied Biosystems) was performed using the SDS software v.2.4 (Applied Biosystems). Relative microRNA abundance was calculated with the RQ Manager v.1.2.1 (Applied Biosystems), and data were analysed with DataAssist v.2.0 (Applied Biosystems).[54] MiRs with cycle threshold (C_t) values $\geqslant 40$ were excluded from further analysis. The expression levels of remaining miRs were calculated against the Ct value of RNU48 as $2^{(-\Delta Ct)}/2^{(-\Delta Ctreference)}$.

Quantitative reverse transcription and real-time PCR

Quantitation of miR-768-3p by qPCR was performed using TaqMan microRNA (Applied Biosystems). Briefly, target miRNA was reverse transcripted from 2 ng purified total miRNA by using TaqMan MicroRNA Reverse Transcription Kit (Applied Biosystems). qPCR was performed using an ABI Fast 7900HT sequence detection system. C_t values for miR-768-3p were normalized to the C_t value of RNU48.

qPCR analysis of eIF4E or AP1G1 mRNA expression was also carried out as described previously.[27] Assay-on-demand for eIF4E (Assay ID: Hs00854166_g1) and for AP1G1 (Assay ID: Hs00964419_m1) were used according to the manufacturer's protocol (Applied Biosystems). The relative expression level of eIF4E mRNA in each sample was normalized against β-actin mRNA.

Plasmid vectors and transfection

The Myc-DDK-tagged ORF clone of eIF4E was purchased from Origene (Australian Biosearch, Perth, WA, Australia). Cells were transfected with 2 μg plasmid or the empty vector in Opti-MEM medium with Lipofectamine 2000 reagent (Invitrogen, Mulgrave, VIC, Australia) according to the manufacturer's protocol.

Overexpression of miR-768-3p

The bacterial stock of Human Pre-microRNA Expression Construct (pCDH-CMV-MCS-EF1-copGFP-miR-768) and the scramble control hairpin in pCDH-CMV-MCS-EF1-copGFP were purchased from System Biosciences (Mountain View, CA, USA). Plasmids were purified by Qiagen Endotoxin-free Plasmid Kit (Qiagen), and were then transfected into cells by Lipofectamine 2000 reagent (Invitrogen) according to the manufacturer's protocol.

Small RNA interference

The siRNA constructs for eIF4E were obtained as the siGENOME SMARTpool reagents from Dharmacon (Thermo Fisher Scientific). The siGENOME SMARTpool eIF4E (M-003884-03-0010) and SiConTRolNontargeting SiRNA pool (D-001206-13-20) were used (Dharmacon).

Luciferase reporter assays

Luciferase report assays to analyse eIF4E-3′-UTR activity was performed as described previously.[22,27] The full-length sequence of eIF4E 3′-UTR is located at the position between 2178 and 4749 of eIF4E mRNA (NM_001968.3). The fragment cloned into the luciferase report plasmid is at a region between 2178 and 3144 of eIF4E mRNA. In brief, eIF4E-3′-UTR and eIF4E-3′-UTR-mut were constructed into pSI-CHECK2-report plasmid (Promega, Sydney, NSW, Australia). Plasmids and miR-768-3p mimics or anti-miR-768-3p were co-transfected into cells (0.5×10^4 cells per well in 96-well plate) by using Lipofectamine 2000 reagent (Invitrogen). The luciferase activity was measured using the Dual Luciferase Reporter Assay System (Promega) and detected by Synergy 2 multidetection microplate reader (BioTek, Winooski, VT, USA) eIF4E 3′-UTR report RNA levels represented by *Renilla* luciferase activity were normalized against luciferase activity of firefly that served as the intraplasmid transfection normalization reporter.

CONFLICT OF INTEREST

The authors declare no conflict of interest.

ACKNOWLEDGEMENTS

This work was supported by the NSW State Cancer Council, Cancer Institute NSW, and National Health and Medical Research Council (NHMRC), Australia. CCJ is a recipient of postdoctoral training Fellowship of NHMRC. XDZ is supported by a senior research fellowship of NHMRC.

REFERENCES

1 Silvera D, Formenti SC, Schneider RJ. Translational control in cancer. *Nat Rev Cancer* 2010; **10**: 254–266.
2 Bilanges B, Stokoe D. Mechanisms of translational deregulation in human tumors and therapeutic intervention strategies. *Oncogene* 2007; **26**: 5973–5990.
3 Grzmil M, Hemmings BA. Translation regulation as a therapeutic target in cancer. *Cancer Res* 2012; **72**: 3891–3900.
4 Bitterman PB, Polunovsky VA. Translational control of cell fate: from integration of environmental signals to breaching anticancer defense. *Cell Cycle* 2012; **11**: 1097–1107.
5 Sonenberg N, Hinnebusch AG. Regulation of translation initiation in eukaryotes: mechanisms and biological targets. *Cell* 2009; **136**: 731–745.
6 Jackson RJ, Hellen CU, Pestova TV. The mechanism of eukaryotic translation initiation and principles of its regulation. *Nat Rev Mol Cell Biol* 2010; **11**: 113–127.
7 Phillips A, Blaydes JP. MNK1 and EIF4E are downstream effectors of MEKs in the regulation of the nuclear export of HDM2 mRNA. *Oncogene* 2008; **27**: 1645–1649.
8 Hou J, Lam F, Proud C, Wang S. Targeting Mnks for cancer therapy. *Oncotarget* 2012; **3**: 118–131.
9 Stumpf CR, Ruggero D. The cancerous translation apparatus. *Curr Opin Genet Dev* 2011; **21**: 474–483.
10 Wendel HG, Silva RL, Malina A, Mills JR, Zhu H, Ueda T *et al.* Dissecting eIF4E action in tumorigenesis. *Genes Dev* 2007; **21**: 3232–3237.
11 Rosenwald IB. The role of translation in neoplastic transformation from a pathologist's point of view. *Oncogene* 2004; **23**: 3230–3247.
12 Larsson O, Li S, Issaenko OA, Avdulov S, Peterson M, Smith K *et al.* Eukaryotic translation initiation factor 4E induced progression of primary human mammary epithelial cells along the cancer pathway is associated with targeted translational deregulation of oncogenic drivers and inhibitors. *Cancer Res* 2007; **67**: 6814–6824.
13 Yang SX, Hewitt SM, Steinberg SM, Liewehr DJ, Swain SM. Expression levels of eIF4E, VEGF, and cyclin D1, and correlation of eIF4E with VEGF and cyclin D1 in multi-tumor tissue microarray. *Oncol Rep* 2007; **17**: 281–287.
14 Coleman LJ, Peter MB, Teall TJ, Brannan RA, Hanby AM, Honarpisheh H *et al.* Combined analysis of eIF4E and 4E-binding protein expression predicts breast cancer survival and estimates eIF4E activity. *Br J Cancer* 2009; **100**: 1393–1399.
15 De Benedetti A, Graff JR. eIF-4E expression and its role in malignancies and metastases. *Oncogene* 2004; **23**: 3189–3199.
16 He L, Hannon GJ 2004MicroRNAs: small RNAs with a big role in gene regulation. *Nat Rev Genet* 2004; **5**: 522–531.
17 Iorio MV, Croce CM. MicroRNAs in cancer: small molecules with a huge impact. *J Clin Oncol* 2009; **27**: 5848–5856.
18 Humphreys DT, Westman BJ, Martin DI, Preiss T. MicroRNAs control translation initiation by inhibiting eukaryotic initiation factor 4E/cap and poly(A) tail function. *Proc Natl Acad Sci USA* 2005; **102**: 16961–16966.
19 Mathonnet G, Fabian MR, Svitkin YV, Parsyan A, Huck L, Murata T *et al.* MicroRNA inhibition of translation initiation *in vitro* by targeting the cap-binding complex eIF4F. *Science* 2007; **317**: 1764–1767.
20 Lujambio A, Lowe SW. The microcosmos of cancer. *Nature* 2012; **482**: 347–355.
21 Felicetti F, Errico MC, Bottero L, Segnalini P, Stoppacciaro A *et al.* The promyelocytic leukemia zinc finger-microRNA-221/-222 pathway controls melanoma progression through multiple oncogenic mechanisms. *Cancer Res* 2008; **68**: 2745–2754.
22 Jin L, Hu WL, Jiang CC, Wang JX, Han CC, Chu P *et al.* MicroRNA-149*, a p53-responsive microRNA, functions as an oncogenic regulator in human melanoma. *Proc Natl Acad Sci USA* 2011; **108**: 15840–15845.
23 Bonazzi VF, Stark MS, Hayward NK. MicroRNA regulation of melanoma progression. *Melanoma Res* 2012; **22**: 101–113.
24 Mueller DW, Bosserhoff AK. The evolving concept of 'melano-miRs'-microRNAs in melanomagenesis. *Pigment Cell Melanoma Res* 2010; **23**: 620–626.
25 Wilmott JS, Zhang XD, Hersey P, Scolyer RA. The emerging important role of microRNAs in the pathogenesis, diagnosis and treatment of human cancers. *Pathology* 2011; **43**: 657–671.
26 Croce CM. Causes and consequences of microRNA dysregulation in cancer. *Nat Rev Genet* 2009; **10**: 704–714.
27 Guo ST, Jiang CC, Wang GP, Li YP, Wang CY, Guo XY *et al.* MicroRNA-497 targets insulin-like growth factor 1 receptor and has a tumour suppressive role in human colorectal cancer. *Oncogene* 2012; **32**: 1910–1920.
28 Davies H, Bignell GR, Cox C, Stephens P, Edkins S, Clegg S *et al.* Mutations of the BRAF gene in human cancer. *Nature* 2002; **417**: 949–954.
29 Platz A, Egyhazi S, Ringborg U, Hansson J. Human cutaneous melanoma; a review of NRAS and BRAF mutation frequencies in relation to histogenetic subclass and body site. *Mol Oncol* 2008; **1**: 395–405.
30 Couts KL, Anderson EM, Gross MM, Sullivan K, Ahn NG. Oncogenic B-Raf signaling in melanoma cells controls a network of microRNAs with combinatorial functions. *Oncogene* 2012; **32**: 1959–1970.
31 Caramuta S, Egyházi S, Rodolfo M, Witten D, Hansson J, Larsson C *et al.* MicroRNA expression profiles associated with mutational status and survival in malignant melanoma. *J Invest Dermatol* 2010; **130**: 2062–2070.
32 Yanagiya A, Suyama E, Adachi H, Svitkin YV, Aza-Blanc P, Imataka H *et al.* Translational homeostasis via the mRNA cap-binding protein, eIF4E. *Mol Cell* 2012; **46**: 847–858.
33 Moerke NJ, Aktas H, Chen H, Cantel S, Reibarkh MY, Fahmy A *et al.* Small-molecule inhibition of the interaction between the translation initiation factors eIF4E and eIF4G. *Cell* 2007; **128**: 257–267.
34 Valleron W, Ysebaert L, Berquet L, Fataccioli V, Quelen C, Martin A *et al.* Small nucleolar RNA expression profiling identifies potential prognostic markers in peripheral T-cell lymphoma. *Blood* 2012; **120**: 3997–4005.
35 Miyoshi K, Miyoshi T, Siomi H. Many ways to generate microRNA-like small RNAs: non-canonical pathways for microRNA production. *Mol Genet Genom* 2010; **284**: 95–103.
36 Arroyo JD, Chevillet JR, Kroh EM, Ruf IK, Pritchard CC, Gibson DF *et al.* Argonaute2 complexes carry a population of circulating microRNAs independent of vesicles in human plasma. *Proc Natl Acad Sci USA* 2011; **108**: 5003–5008.
37 Kiss T. Biogenesis of small nuclear RNPs. *J Cell Sci* 2004; **117**: 5949–5951.
38 Rosenwald IB, Rhoads DB, Callanan LD, Isselbacher KJ, Schmidt EV. Increased expression of eukaryotic translation initiation factors eIF-4E and eIF-2 alpha in response to growth induction by c-myc. *Proc Natl Acad Sci USA* 1993; **90**: 6175–6178.
39 Mamane Y, Petroulakis E, Martineau Y, Sato TA, Larsson O, Rajasekhar VK *et al.* Epigenetic activation of a subset of mRNAs by eIF4E explains its effects on cell proliferation. *PLoS One* 2007; **2**: e242.
40 Rosenwald IB, Lazaris-Karatzas A, Sonenberg N, Schmidt EV. Elevated levels of cyclin D1 protein in response to increased expression of eukaryotic initiation factor 4E. *Mol Cell Biol* 1993; **13**: 7358–7363.
41 Koromilas AE, Lazaris-Karatzas A, Sonenberg N. mRNAs containing extensive secondary structure in their 5′ non-coding region translate efficiently in cells overexpressing initiation factor eIF-4E. *EMBO J* 1992; **11**: 4153–4158.
42 Lazaris-Karatzas A, Montine KS, Sonenberg N. Malignant transformation by a eukaryotic initiation factor subunit that binds to mRNA 5′ cap. *Nature* 1990; **345**: 544–547.
43 Lazaris-Karatzas A, Sonenberg N. The mRNA 5′ cap-binding protein, eIF-4E, cooperates with v-myc or E1A in the transformation of primary rodent fibroblasts. *Mol Cell Biol* 1992; **12**: 1234–1238.
44 Graff JR, Konicek BW, Carter JH, Marcusson EG. Targeting the eukaryotic translation initiation factor 4E for cancer therapy. *Cancer Res* 2008; **68**: 631–634.
45 Bemis LT, Chen R, Amato CM, Classen EH, Robinson SE, Coffey DG *et al.* MicroRNA-137 targets microphthalmia-associated transcription factor in melanoma cell lines. *Cancer Res* 2008; **68**: 1362–1368.
46 Haflidadóttir BS, Bergsteinsdóttir K, Praetorius C, Steingrímsson E. miR-148 regulates Mitf in melanoma cells. *PLoS One* 2010; **5**: e11574.
47 Li SC, Tang P, Lin WC. Intronic MicroRNA: Discovery and biological implications. *DNA Cell Biol* 2007; **26**: 195–207.
48 Takatsu H, Sakurai M, Shin HW, Murakami K, Nakayama K. Identification and characterization of novel clathrin adaptor-related proteins. *J Biol Chem* 1998; **273**: 24693–24700.
49 Hong DS, Kurzrock R, Oh Y, Wheler J, Naing A, Brail L *et al.* A phase 1 dose escalation, pharmacokinetic, and pharmacodynamic evaluation of eIF-4E antisense oligonucleotide LY2275796 in patients with advanced cancer. *Clin Cancer Res* 2011; **17**: 6582–6591.
50 Ibrahim AF, Weirauch U, Thomas M, Grünweller A, Hartmann RK, Aigner A. MicroRNA replacement therapy for miR-145 and miR-33a is efficacious in a model of colon carcinoma. *Cancer Res* 2011; **71**: 5214–5224.
51 Jiang CC, Lai F, Tay KH, Croft A, Rizos H, Becker TM *et al.* Apoptosis of human melanoma cells induced by inhibition of B-RAFV600E involves preferential splicing of bimS. *Cell Death Dis* 2010; **2**: 1:e69.
52 Dong L, Jiang CC, Thorne RF, Croft A, Yang F, Liu H *et al.* Ets-1 mediates upregulation of Mcl-1 downstream of XBP-1 in human melanoma cells upon ER stress. *Oncogene* 2011; **30**: 3716–3726.
53 Blais JD, Filipenko V, Bi M, Harding HP, Ron D, Koumenis C *et al.* Activating transcription factor 4 is translationally regulated by hypoxic stress. *Mol Cell Biol* 2004; **24**: 7469–7482.
54 Wulfken LM, Moritz R, Ohlmann C, Holdenrieder S, Jung V, Becker F *et al.* MicroRNAs in renal cell carcinoma: diagnostic implications of serum miR-1233 levels. *PLoS One* 2011; **6**: e25787.

Supplementary Information accompanies this paper on the Oncogene website (http://www.nature.com/onc)